Multivariate fMRI and Eye Tracking Reveal Differential Effects of Visual Interference on Recognition Memory Judgments for Objects and Scenes

Edward B. O'Neil[1*], Hilary C. Watson[1*], Sonya Dhillon[1], Nancy J. Lobaugh[1,2], and Andy C. H. Lee[1,3]

Abstract

■ Recent work has demonstrated that the perirhinal cortex (PRC) supports conjunctive object representations that aid object recognition memory following visual object interference. It is unclear, however, how these representations interact with other brain regions implicated in mnemonic retrieval and how congruent and incongruent interference influences the processing of targets and foils during object recognition. To address this, multivariate partial least squares was applied to fMRI data acquired during an interference match-to-sample task, in which participants made object or scene recognition judgments after object or scene interference. This revealed a pattern of activity sensitive to object recognition following congruent (i.e., object) interference that included PRC, prefrontal, and parietal regions. Moreover, functional connectivity analysis revealed a common pattern of PRC connectivity across interference and recognition conditions. Examination of eye movements during the same task in a separate study revealed that participants gazed more at targets than foils during correct object recognition decisions, regardless of interference congruency. By contrast, participants viewed foils more than targets for incorrect object memory judgments, but only after congruent interference. Our findings suggest that congruent interference makes object foils appear familiar and that a network of regions, including PRC, is recruited to overcome the effects of interference. ■

INTRODUCTION

Adaptive behavior relies upon the encoding of relevant information in the environment and the selective retrieval of that information when needed. The richness of human experience, however, presents a significant computational challenge to the capacity-limited neural systems supporting these processes. Irrelevant information can lead to proactive as well as retroactive interference, and although neurologically healthy individuals are generally quite adept at ameliorating the effects of this interference, failures in interference resolution do occur, leading to cognitive errors. Such failures can become more common and exacerbated following brain damage, and it has been suggested that interference can be a significant factor underlying the pervasive loss of memory in individuals with organic amnesia (Saksida & Bussey, 2010; Cowan, Beschin, & Della Sala, 2004; Warrington & Weiskrantz, 1970). It is, therefore, a clinically and ecologically important challenge for cognitive neuroscience to understand how the brain resolves interference in the context of mnemonic processing.

In visual object recognition memory, interference can arise when target and lure items share visual features. Computationally, it has been demonstrated that access to representations that are highly integrated at the feature level can aid in resolving visual interference. At this level of representation, lure stimuli fail to reactivate the specific co-occurrence of features diagnostic to the target object, even when they possess some visual features common to the target (Cowell, Bussey, & Saksida, 2006, 2010; Bussey & Saksida, 2002). The perirhinal cortex (PRC), a medial-temporal lobe (MTL) region, has been suggested to be critical for object representations that are highly resilient to feature interference (Cowell et al., 2010; Saksida & Bussey, 2010; Murray, Bussey, & Saksida, 2007). According to this view, object recognition deficits can arise in rodents and humans with PRC damage because of an inability to resolve interference that is a consequence of ongoing perceptual processing, and subsequently such recognition impairments can be reduced when interference is curtailed before retrieval. In support of this, McTighe, Cowell, Winters, Bussey, and Saksida (2010) reported that recognition deficits following PRC lesions were eliminated when rodents were placed in a dark holding cage during the delay period of a modified spontaneous object recognition task. This finding is consistent with the prediction that minimizing perceptual

[1]University of Toronto, Ontario, Canada, [2]Centre for Addiction and Mental Health, Toronto, Ontario, Canada, [3]Baycrest Centre for Geriatric Care, Toronto, Ontario, Canada
*These authors contributed equally to this work.

Journal of Cognitive Neuroscience 27:9, pp. 1708–1722
doi:10.1162/jocn_a_00816

interference by prohibiting visual processing of the environment during the delay can reduce impairments related to PRC damage. Similarly, PRC-lesioned rats were found to be impaired at object recognition when interfering objects resembled targets but not when interfering stimuli were perceptually dissimilar to the target (Bartko, Cowell, Winters, Bussey, & Saksida, 2010). Finally, in humans, patients with extensive MTL damage that included the PRC were impaired at object discrimination following presentation of high, but not low, object feature interference (Barense et al., 2012).

Using fMRI in healthy individuals, we recently examined the consequences of visual interference on PRC involvement during memory retrieval. A novel interference match-to-sample (IMTS) paradigm (Watson & Lee, 2013) was used to assess object and scene memory following periods of visual interference. For each trial, participants were first required to encode an object-in-scene image. Following a period of object or scene visual interference, memory for an aspect of the target image (either the object or scene) was assessed using a two-alternative forced-choice task. Activity was reliably greater in PRC following a period of object compared with scene interference, but only during object memory retrieval. By contrast, interference-related modulations in PRC activity were not observed for scene recognition. These PRC effects were accompanied by similar interference-related differences in match-to-sample (MTS) memory performance; object MTS was worse following congruent (object), as compared to incongruent (scene) interference. The hippocampus, however, was found to play a domain general role in interference resolution. Such a role of the hippocampus in interference resolution is consistent with other domain-general functions linked to this structure, such as pattern separation/completion, match/mismatch sensitivity, and associative/relational binding, in addition to more recent work linking the hippocampus to memory for temporal information (Howard & Eichenbaum, 2013; Yassa & Stark, 2011; Davachi, 2006; Kumaran & Maguire, 2006; Eichenbaum, 2004).

Although the findings of Watson and Lee (2013) provided valuable insight into PRC activity during interference resolution, extra-MTL contributions to the IMTS task were not examined. Beyond the MTL, PFC-mediated processes are known to support retrieval when conditions of high interference occur and/or bottom–up processes fail to automatically activate the appropriate representation (Badre, Poldrack, Paré-Blagoev, Insler, & Wagner, 2005; Badre & Wagner, 2002). In particular, the dorsolateral (DLPFC) and ventrolateral (VLPFC) prefrontal cortices have been suggested to subserve proactive control strategies that are necessary for successful memory retrieval, including controlled (or active) retrieval and postretrieval selection (Badre & Wagner, 2002, 2007; Badre et al., 2005; Fletcher & Henson, 2001). Although evidence for distinctions along the dorsal/ventral axis of lateral PFC is not as strong as that for the rostral/caudal axis (Blumenfeld, Nomura, Gratton, & D'Esposito, 2013), it has been proposed that DLPFC supports control processes relevant to the organization of multiple pieces of information in support of current goals, including relational processing, manipulation, and monitoring of goal-relevant information. In contrast, the VLPFC has been implicated in first-order cognitive control processes related to item processing, including selection/updating, maintenance, and retrieval of goal-relevant information (Blumenfeld et al., 2013; Blumenfeld & Ranganath, 2007; see also Fletcher & Henson, 2001). With respect to VLPFC, it has been proposed that subdivisions within this region may make distinct contributions to retrieval-related processes with controlled retrieval of relevant representations proposed to rely on the anterior VLPFC, whereas postretrieval selection is proposed to rely on the mid-VLPFC (see Badre & Wagner, 2007, for a review). Controlled retrieval involves the maintenance of current retrieval objectives (Badre & Wagner, 2007; Tomita, Ohbayashi, Nakahara, Hasegawa, & Miyashita, 1999) and the activation of long-term representations stored in the temporal cortices (Thompson-Schill, D'Esposito, Aguirre, & Farah, 1997) to bias recovery of goal-relevant information. Because the latter can often activate large amounts of conflicting and unsuitable information (Badre et al., 2005; Anderson & Spellman, 1995), postretrieval selection is then critical to monitor the quality of activated mnemonic representations and deliver an appropriate response (Badre & Wagner, 2007; Nee, Jonides, & Berman, 2007). Beyond the lateral PFC, the ACC has been associated with the detection of response conflict (Milham & Banich, 2005; Milham et al., 2002; MacDonald, Cohen, Stenger, & Carter, 2000; Pardo, Pardo, Janer, & Raichle, 1990) and, in conjunction with posterior parietal cortices (PPC), bringing focus to the necessary representation/item for response selection (Nee, Wager, & Jonides, 2007; Bunge, Hazeltine, Scanlon, Rosen, & Gabrieli, 2002; Durston, Thomas, Worden, Yang, & Casey, 2002; de Zubicaray, McMahon, Wilson, & Muthiah, 2001; MacDonald et al., 2000; Praamstra, Kleine, & Schnitzler, 1999; Iacoboni, Woods, & Mazziotta, 1998) and maintaining this focus until response execution is complete (Johnson et al., 2005).

It would appear, therefore, that PFC- and PPC-mediated processes work in unison to resolve memory interference. If this is the case, it is conceivable that object-specific interference-related memory failures may occur because PRC-dependent object representations become essential following object interference to disambiguate targets from foils but are not made available and/or selected by higher-order control processes. Although previous investigations have examined functional connectivity between the MTL and broader cortical networks, there is little existing research that specifically addresses how the MTL works in concert with the broader network of regions in support of the retrieval and selection of information under conditions of visual interference. Instead, previous studies examining MTL/PFC connectivity have

largely focused on word stimuli (e.g., Barredo, Öztekin, & Badre, 2015; Axmacher, Schmitz, Wagner, Elger, & Fell, 2008), and when visual stimuli have been examined, connectivity has been investigated in the context of encoding, rather than retrieval (e.g., Ranganath & D'Esposito, 2005), or in the absence of a visual interference manipulation (e.g., McCormick, Moscovitch, Protzner, Huber, & McAndrews, 2010). Thus, the nature of MTL connectivity under changing visual interference demands at retrieval has remained largely unexamined. The first aim of the current study was, therefore, to examine the interplay between the PRC and PFC/PPC regions supporting controlled retrieval. To address this, we applied a covariance-based multivariate approach, known as partial least squares (PLS; McIntosh & Lobaugh, 2004; McIntosh, Bookstein, Haxby, & Grady, 1996) to the data from our previous fMRI investigation (Watson & Lee, 2013). This analysis allowed the identification of whole-brain patterns of interference-related activity during retrieval and the assessment of functional connectivity between these regions and the PRC across the various IMTS task conditions. Given our univariate findings, we predicted that these analyses would reveal PRC sensitivity to object memory following congruent (object) interference. More critically, this pattern should also be evident in PFC and PPC regions, reflecting the interaction between PRC representations and regions supporting processes necessary following interference, such as controlled retrieval and postretrieval selection. As PFC/PPC regions support interference resolution via these stimulus nonspecific processes, the observed interregional correlations between PRC and PFC/PPC may be agnostic to the type of recognition memory and interference involved.

One further question arising from Watson and Lee (2013) relates to the nature of the information used to support IMTS performance. Specifically, performance on each trial could reflect the recognition of the target or correct rejection of the foil. Given the two-alternative forced-choice nature of the task, differentiating between these two possibilities using RT or behavioral accuracy is not feasible. One method that can shed light on this issue is eye tracking, as this technique allows the collection of separate viewing time data for concurrently presented stimuli. As target and foil stimuli are presented simultaneously during the recognition phase of the IMTS trial, eye tracking can provide insight into the nature of information attended during retrieval. Growing evidence suggests that incidental eye movements can elucidate the contributions of representations to recognition memory, which would otherwise be inaccessible via explicit measures alone (Hannula & Ranganath, 2008; Holm, Eriksson, & Andersson, 2008; Hannula, Ryan, Tranel, & Cohen, 2007; Ryan, Hannula, & Cohen, 2007). Furthermore, recent studies have found that eye movements can provide insight into the impact of feature interference on recognition memory. For instance, eye movements have been shown to reflect the similarity of the foils to the target and have been used to track the degradation of a representation over time (Yeung, Ryan, Cowell, & Barense, 2013; Warren, Duff, Tranel, & Cohen, 2011). Thus, eye movements provide a promising measure to further understand recognition processes under different interference conditions.

The second aim of the current study was, therefore, to examine gaze duration for target and foil stimuli during the IMTS task. To achieve this, we tested a new group of participants on the IMTS paradigm (Watson & Lee, 2013) and monitored eye movements during object and scene recognition, following object or scene interference. Complementary to the pattern of explicit IMTS performance from our previous study, we expected that eye movements should relate to the changing conditions of memory interference. Furthermore, interference-related eye movements should provide an early index of memory failure/success, whereby enhanced viewing of foil information will precede incorrect responses. This is because eye movements should implicitly reflect a combination of increased familiarity for foil information following exposure to similar interfering features and the failure to activate a sufficiently complex representation given this feature ambiguity. As such, we predicted that participants would look disproportionately at foil objects before making incorrect MTS judgments following periods of congruent interference.

METHODS

Functional Neuroimaging Study

Participants

Twenty-five volunteers were recruited via posted advertisements on the campus of the University of Oxford. All participants were right-handed, with normal or corrected-to-normal vision and no history of neurological and/or psychiatric disorders. Participants gave written informed consent before the experiment and were compensated £10/hr. One participant was removed from all analyses as they were unable to complete all three scans and had poor behavioral performance on those completed ($z < -2.5$). The mean age of the remaining 24 participants (12 women) was 22.9 years (range = 19–30 years). The experiment received ethical approval from the Oxfordshire Research Ethics Committee A (Ref: 07/H0604/115).

Experiment Design

The methods for the fMRI study have been described previously in Watson and Lee (2013). The experiment consisted of three fMRI runs of a novel IMTS task. Each IMTS trial required the participant to study an image and, following a period of visual interference, identify which of two images was the target (studied) image. Object-in-scene images were presented in all phases of the experiment (i.e., images of real-world objects superimposed on virtual

reality scenes). In the study phase of each trial, the target stimulus was presented on the screen for 2800 msec. Participants were explicitly instructed to encode the object and the scene. Following a brief (200-msec) ISI, a visual interference phase was presented, consisting of a series of seven rapidly displayed object-in-scene images, each shown for 350 msec with a 250-msec ISI. These images were similar to the target image but differed with respect to either object (object interference condition) or scene (scene interference condition) content, whereas content in the other domain was identical to the studied item. Interfering objects were of the same semantic category as the target (for an example, see Figure 1), whereas interfering scenes had similar colors and features but varied in spatial layout and viewpoint. To ensure that participants were attending to interfering stimuli, a 1-back stimulus repetition was present during each interference phase. Participants were required to indicate this repetition using an MR-compatible button box held in the right hand.

The end of the interference phase was marked by a jittered ISI (mean = 4000 msec), which was followed by the test phase of the trial. Participants were presented with a pair of images shown for 3700 msec. One of these two stimuli was the original study image (i.e., the target), and the other differed from the target (i.e., the foil). Scene or object memory was assessed through the characteristics of the foil stimulus, which either comprised a visually similar object from the same semantic category (i.e., clock) overlaid on the original scene (object recognition, OR) or the same object as the target, with a novel, but visually similar scene (scene recognition, SR). Participants indicated whether the target was presented on the left or right of the display by pressing the corresponding response button. At the end of the test phase, there was a variable intertrial interval (mean = 4000 msec). Critical to the experimental design, the domain of visual interference (object or scene) was independent of the domain to be discriminated at test. Thus, participants were naive to the type of memory (object or scene) being assessed until the test phase of the trial, requiring encoding and maintenance of both types of information. This design allowed the differential impact of object and scene interference on object and scene recognition memory to be assessed. Our two interference and recognition types resulted in a total of four conditions of interest: two congruent interference conditions (object recognition–object interference [OROI] and scene recognition–scene interference [SRSI]) and two incongruent interference conditions (object recognition–scene interference [ORSI] and scene recognition–object interference [SROI]). A third type of interference (scrambled images) was also included, but as this condition did not directly address our current goal of comparing spatial and object interference, these trials were excluded from the behavioral and imaging analyses (as in Watson & Lee, 2013). There were 36 IMTS trials for each experimental condition, resulting in 144 total trials, 48 per run. Trials within runs were presented in a pseudorandom order, and the order of the three runs within each testing session was counterbalanced across participants. In addition, to ensure participants understood task instructions, a practice phase containing eight IMTS trials (two per condition) was administered before the experimental task.

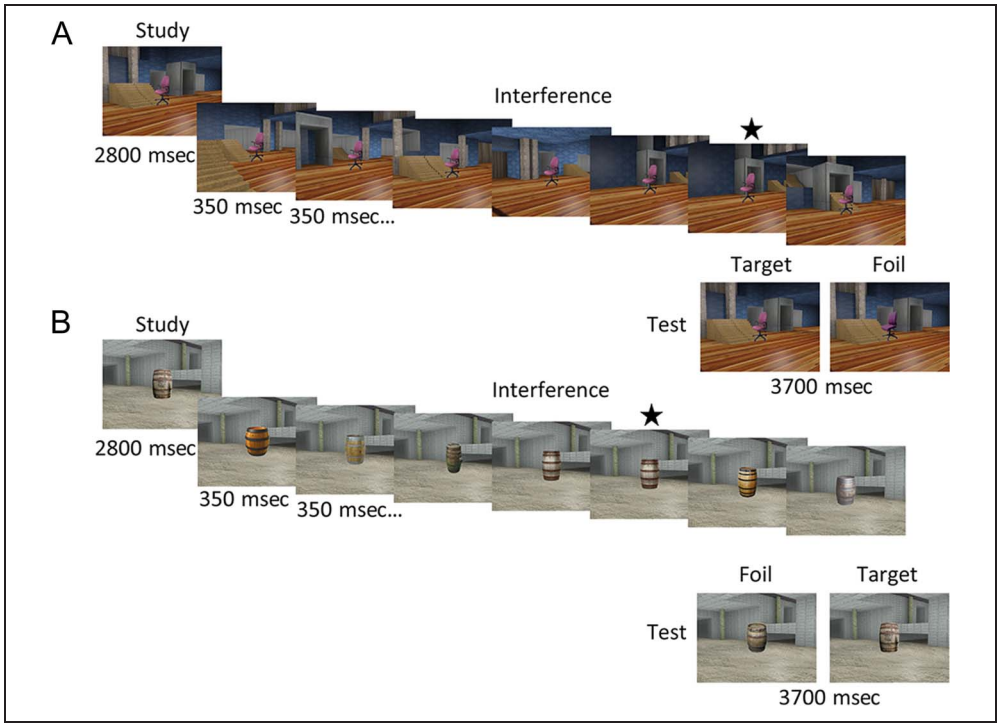

Figure 1. Example trials from (A) ORSI and (B) OROI conditions (SRSI and SROI not shown). All IMTS trials were composed of a study, interference, and test phase. At study, a target image was presented, followed by a 200-msec ISI. During the interference phase, participants were required to detect an image repetition (indicated by the black stars) while a series of seven interfering stimuli were presented (differing in either scene or object content, i.e., scene or object interference). At test, participants indicated which of two simultaneously presented images (differing in item or scene content, i.e., object or scene recognition) was the target image.

Scanning Procedure

Scanning was performed using a Siemens Magnetom Verio 3T MRI system (Erlangen, Germany) and a gradient-echo EPI sequence. Forty-three slices were collected per image volume (2.0 mm thickness, interslice distance 0.5 mm, in-plane resolution 3 × 3 mm, repetition time [TR] = 2400 msec, echo time [TE] = 30 msec, flip angle [FA] = 78°, field of view [FOV] = 192 × 192 × 107 mm). Slices were acquired in a descending order, with an oblique axial tilt relative to the anterior–posterior commissure line (posterior downward) to prevent image ghosting and to maximize coverage of the temporal lobe. Each EPI session was approximately 20 min in duration, which included four dummy scans at the start of the scanning run to allow the MR signal to reach equilibrium. To correct for geometric distortions in the EPI data because of magnetic field inhomogeneity, a map of the magnetic field was produced from two 3-D FLASH images acquired during the scanning session (Jezzard & Balaban, 1995; TE = 5.19 and 7.65 msec, TR = 430 msec, and FA = 60°), with an acquisition plane identical to the EPI data. Anatomical images were acquired using a standard T1-weighted sequence comprising 178 axial slices (3-D FSPGR; TR = 2040 msec, TE = 4.7 msec, FA = 8°; FOV = 192 × 174 × 192 mm, and 1 mm isotropic resolution).

Data Preprocessing

Functional imaging data were preprocessed using FEAT (fMRI Expert Analysis Tool Version 5.98, which is part of FSL [FMRIB Software Library], www.fmrib.ox.ac.uk/fsl; Smith et al., 2004) in the following manner: (1) motion correction using MCFLIRT (Jenkinson, Bannister, Brady, & Smith, 2002), (2) unwarping of the EPI data using the acquired field maps and PRELUDE + FUGUE (Jenkinson, 2003) to correct for image distortions arising from magnetic field inhomogeneities, (3) segmentation of brain from nonbrain matter using a mesh deformation approach (BET; Smith, 2002), (4) spatial smoothing using a Gaussian kernel of FWHM 6.0 mm, (5) grand mean intensity normalization of the entire 4-D data by a single multiplicative factor, (6) high-pass temporal filtering using Gaussian-weighted least squares straight line fitting with sigma = 50 sec, (7) independent component analysis to identify and remove any noise artifacts (MELODIC; Beckmann & Smith, 2004), and finally (8) registration of the EPI data to high resolution 3-D anatomical T1 scans (per participant) and to a standard Montreal Neurological Institute (MNI-152) template image using a combination of FLIRT and FNIRT (Jenkinson et al., 2002; Jenkinson & Smith, 2001).

PLS Analysis

Following preprocessing, the functional imaging data were submitted to PLS analysis to define differences among the task conditions (task PLS; McIntosh & Lobaugh, 2004; McIntosh et al., 1996). PLS is a covariance-based multivariate analysis technique that examines how patterns of activity vary across the brain over time as a function of task conditions. As PLS does not rely on assumptions about the shape of the hemodynamic response function (HRF), distributed whole-brain changes in activity across conditions can be measured with greater sensitivity than a standard univariate approach (McIntosh & Lobaugh, 2004). Moreover, as the PLS analyses employed here are model-free, we were able to identify spatial-temporal patterns of activity in a data-driven manner.

The time course data were extracted as a difference measure from the retrieval stimulus onset for five discrete 2400 msec "lags" (i.e., TRs), resulting in a 12-sec window capturing the hemodynamic response. The mean response at each lag for all conditions was extracted for all voxels such that four vectors representing the mean time course across the whole brain were created for each participant. For task PLS, a task deviation matrix was made by removing the grand mean and averaging the deviation scores within condition (McIntosh & Lobaugh, 2004). This deviation matrix was subjected to singular-value decomposition resulting in a set of orthogonal latent variables (LVs) that describe the relation between the design and data matrices. Each LV was composed of (1) a singular-value indicating the strength of the LV, (2) a linear contrast between the task conditions coding the effect depicted by the LV, and (3) a singular image detailing the weight or "salience" of each voxel to the LV within each time lag proportional to the covariance of activity with the contrast. The statistical significance of each LV was formally assessed via a permutation technique that randomly reassigned each participant's data to each condition before rerunning the analysis. With each reordering a new singular value is created, and in the current analysis this reordering was carried out 500 times (i.e., 500 permutations). As such, the significance for a given LV reflects the exact probability that the singular value from the permuted data exceeded the original LV singular value, applying a threshold of $p < .05$ (Stevens, Hasher, Chiew, & Grady, 2008).

The reliability of the LV voxel saliences from the singular image was established using bootstrap estimation of the standard error (*SE*). Specifically, this procedure involved randomly resampling participants with replacement and rerunning the PLS analysis to determine new saliences. For this study, this bootstrap procedure was repeated 100 times, and the bootstrap *SE* was calculated from the resampled saliences. As the ratio of the observed salience to the bootstrap *SE* approximates a *z* score, clusters comprising five or more voxels with a bootstrap ratio (BSR) greater than 2.81 were considered reliable. Findings from the aforementioned task PLS analysis were then used to examine PRC functional connectivity via seed PLS employing a statistical inference approach identical to that adopted for task PLS. Full details of this approach are described in the Results section.

Eye-tracking Study

Participants

Twenty-three participants (14 women) aged 17–23 years (mean = 19.1 years) were recruited from the undergraduate research pool at the University of Toronto Scarborough. Participants had normal or corrected-to-normal vision and no history of neurological or psychiatric disorders. All participants provided written informed consent and received course credit for their participation. The experiment received ethical approval from the University of Toronto Office of Research Ethics Protocol (reference number: 26827).

Eye-tracking Procedure

The experimental paradigm was identical to that used in the fMRI study described above with the following exceptions. To ensure gaze position began at the same central location of the screen on every IMTS trial, participants were required to fixate on a crosshair presented in the center of the display for 1000 msec before each trial. The intertrial interval was fixed at 4000 msec, and rather than a MR compatible button box, a button press on a keyboard was used to collect participant responses. Finally, the scrambled interference condition (which was not included in the analysis of Watson & Lee, 2013) was removed, as it did not directly address the goal of comparing spatial and object interference.

A Tobii T120 eye tracker (Tobii Technology, Danderyd, Sweden), which consists of a 17-in. LCD monitor with an integrated 120-Hz eye tracker, was used to conduct the experiment. This system was connected to a laptop PC running E-Prime (Psychology Software Tools, Pittsburgh, PA) and the Tobii Studio software program for administration of the experimental task and recording eye movements and behavioral data. Participants were seated approximately 15 cm from the eye-tracking system and were instructed to keep their heads as still as possible. At the beginning of each experimental run, the eye tracker was recalibrated to ensure accurate recordings over the course of the experimental session.

Eye-tracking Analysis

As the goal of the eye-tracking study was to assess the effects of interference during recognition memory decisions, trial-specific time windows were created from the onset of the recognition phase (the presentation of the target and foil stimuli) up until participant response. Percent viewing time (PVT) was calculated separately for each trial. After accounting for eye blinks, gaze duration within predefined areas of interest in the visual display was calculated. For object recognition trials, these comprised the target object, the foil object, and the remainder of the display. For scene recognition trials, the area of interest comprised the target scene, the foil scene, and the remainder of the display. To simplify the data analysis, target viewing bias (target PVT–foil PVT) was used as the dependent measure of interest. This bias was calculated separately for accurate and inaccurate trials from each of the four IMTS conditions for each participant. These values were then assessed at the group level to investigate the consequences of congruent and incongruent visual interference on target viewing, separately for accurate and inaccurate trials, as well as the two recognition memory conditions. A few participants did not commit an error in some conditions, subsequently excluding them from certain analyses, as indicated by the degrees of freedom reported.

RESULTS

Functional Neuroimaging Study

Behavioral Data

As previously reported in Watson and Lee (2013), memory and interference conditions were found to interact (Memory × Interference interaction, $F(1, 23) = 87.37$, $p < .001$) such that performance was reduced under conditions of congruent as compared to incongruent conditions (OROI < ORSI: $t(23) = 9.56$, $p < .001$; SRSI < SROI $t(23) = 4.26$, $p < .001$). For comparison with the accuracy data of the eye-tracking study, the means and standard deviations for the experimental conditions were as follows *M*(*SEM*): OROI = .80(.02); ORSI = .95(.01); SRSI = .86(.02); SROI = .90(.01). The 1-back task during the interference phase was employed to ensure participants attended to the stimuli. The proportion of correctly identified repeating stimuli (hits; H) and novel stimuli incorrectly identified as repeats (false alarms; FA) were calculated for each recognition/interference condition. d' scores were calculated from these H and FA rates as a measure of working memory accuracy (d' = Z(H) − Z(FA)). Performance on the 1-back task was quite good across conditions ($d' > 1$), with greater accuracy for object interference conditions than scene interference conditions ($t(23) = 6.38$, $p < .001$). For comparison with the accuracy data of the eye-tracking study, the means and standard deviations for the experimental conditions were as follows *M*(*SEM*): OROI = 3.36(.13); ORSI = 2.53(.14); SRSI = 2.35(.11); SROI = 2.53(.14).

Neuroimaging Data

A two-stage PLS approach was employed. First, accurate trials were examined using data-driven task PLS analysis to identify spatial-temporal patterns of brain activity that reflected a differential sensitivity to object recognition following congruent in comparison to incongruent interference. Given the findings of Watson and Lee (2013), we predicted that this analysis would reveal PRC activity as well as activity in other regions linked to memory and attention in the support of interference resolution, such as DLPFC, VLPFC, ACC, and PPC (see Introduction). Second, we used seed PLS to assess whether the functional

connectivity between PRC and those regions identified with task PLS varied significantly across the different interference conditions. Again, analyses were restricted to accurate trials.

The task PLS analysis identified two significant patterns of brain activity or LVs that differentiated our IMTS conditions. The first LV ($p < .001$) differentiated conditions by interference type (SI > OI; Figure 2A). Interestingly, inspection of the 95% confidence intervals in Figure 2A reveals this distinction was not driven by high (congruent) interference conditions. Rather, this distinction was primarily driven by low (incongruent) interference conditions. As can be seen in Figure 2B, during object recognition following scene interference involvement of lateral ventral temporal cortex, VLPFC, ACC/anterior midline regions, and the hippocampus was elevated, whereas activity was reduced in posterior parahippocampal gyrus, retrosplenial cortex, and posterior DLPFC. The converse was true during scene recognition following object interference. As incongruent interference conditions were also associated with increased behavioral recognition performance, object and scene-related activity linked to incongruent interference conditions may reflect greater access to information in the relevant domain during retrieval.

The second LV ($p < .02$) broadly differentiated object and scene recognition conditions (Figure 3). Whereas cool regions, reflecting greater activation during the scene recognition than object recognition conditions, were not differentiated by interference demands (as indicated by overlapping 95% confidence intervals in Figure 3A), warm regions, reflecting greater activation during object than scene recognition conditions, exhibited more reliable activation under conditions of congruent rather than incongruent interference, suggesting that this pattern of regions was differentially engaged depending on the type of interference experienced. This differential sensitivity to interference demands, specific to the object recognition condition (i.e., OROI > ORSI; SROI = SRSI), closely resembles the object memory interference-related PRC activity identified using a univariate analysis approach (Watson & Lee, 2013). Regions exhibiting reliable positive saliences (BSR > 2.81) for the pattern depicted by LV2 are indicated by warm colors in Figure 3B. Critically, reliable clusters of activity were evident in the left PRC region at Lag 3 (−32, −10, −38; BSR 3.11; see Figure 4A) in a location proximal to that previously revealed to exhibit selective effects in the OROI condition (Watson & Lee, 2013) and a region anterior to this during Lag 1 (−26, 4, −26; BSR = 3.66). Several other predicted regions relevant for interference resolution were also part of this pattern (Figure 4B). These positive saliences peaked during Lag 1 in the hippocampus (28, −18, −6; BSR = 4.17), Lag 3 in the anterior (44, 28, 10; BSR = 4.73) and mid VLPFC (−48, 14, 16; BSR = 4.60), Lag 4 in the rostral PFC (40, 48, −8; BSR = 5.38), and Lag 5 in the DLPFC (38, 32, 44; BSR = 4.62), ACC (0, 8, 54; BSR = 4.18), and PPC (−18, −70, 34; BSR = 5.87).

The pattern identified in LV2 indicated coinvolvement of PRC and other regions during the object recognition task following congruent interference, a pattern that

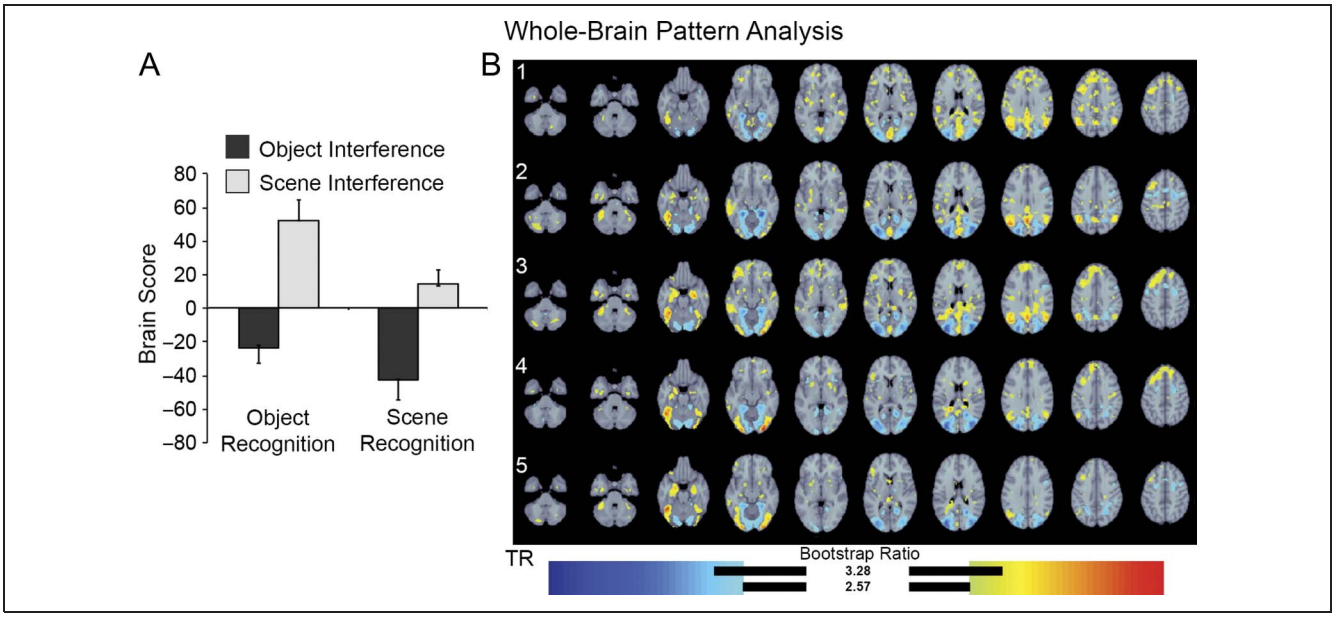

Figure 2. Data-driven PLS findings. (A) Brain scores associated with the latent variable (LV1) differentiating object and scene interference conditions. Note that incongruent interference conditions (ORSI and SROI) primarily contribute to this distinction (error bars = 95% CI). (B) Spatiotemporal pattern of correlations relating to the task distinction shown in (A). Warm colors reflect increased activity during scene interference as compared with object interference conditions, whereas cool colors reflect the converse pattern. Rows reflect TRs from the onset of the test phase capturing the duration of the HRF. Statistical map thresholded at BSR = 2.57 for presentation purposes. Brain images displayed using neurological convention (Left = Left).

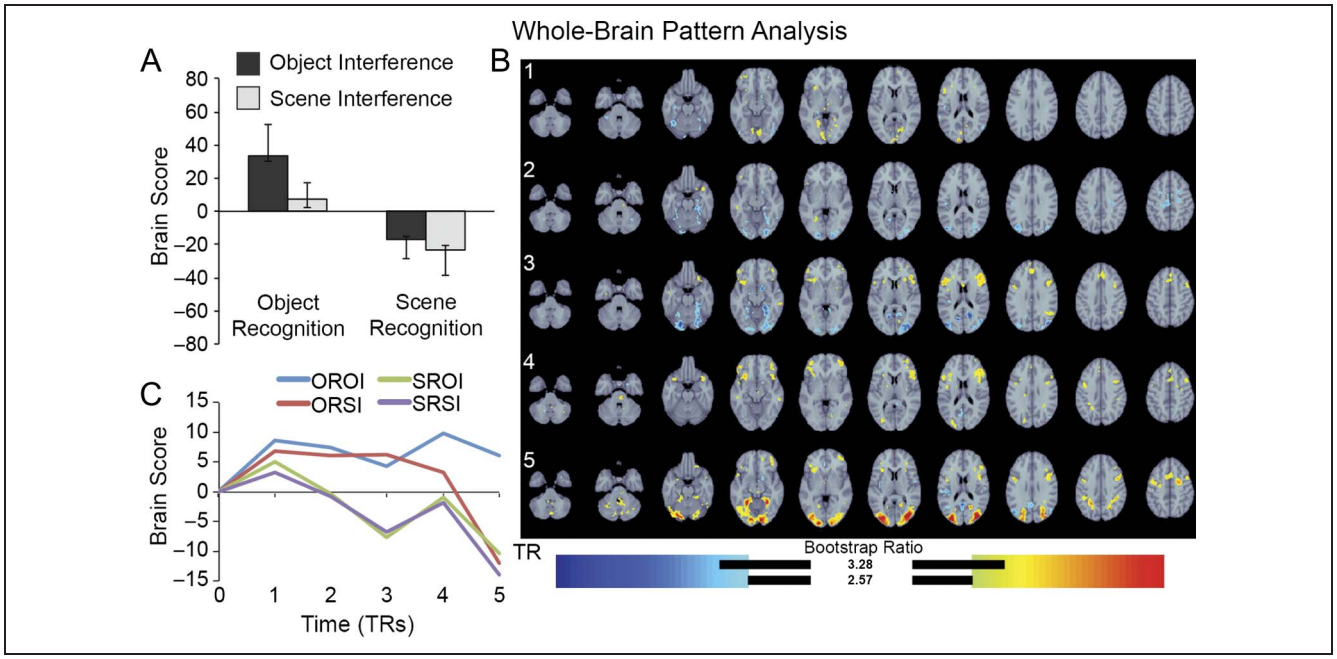

Figure 3. Data-driven PLS findings. (A) Brain scores associated with the latent variable (LV2) differentiating object and scene recognition conditions. Note that the object interference conditions make a stronger contribution to the former (error bars = 95% CI). (B) Spatiotemporal pattern of correlations relating to the task distinction shown in (A). Warm colors reflect a pattern of increased activity during the object recognition task as compared with the scene recognition task, whereas cool colors reflect the converse pattern. Rows reflect TRs from the onset of the test phase capturing the duration of the HRF. (C) Temporal brain scores demonstrating the temporal development of the distinction of object and scene recognition conditions over time. Statistical map thresholded at BSR = 2.57 for presentation purposes. Brain images displayed using neurological convention (Left = Left).

mirrored our original univariate findings (reported in Watson & Lee, 2013). Moreover, LV2 exhibited reliable voxel saliences (BSR > 2.81) in a number of predicted brain regions known to contribute to interference resolution, including the VLPFC, DLPFC, ACC, and PPC. In the second step of the analysis, we investigated the functional connectivity between PRC and other regions that were part of LV2 using seed PLS. A PRC seed region was defined functionally by extracting the average response from Lag 3 (associated with the peak of the HRF) for each participant

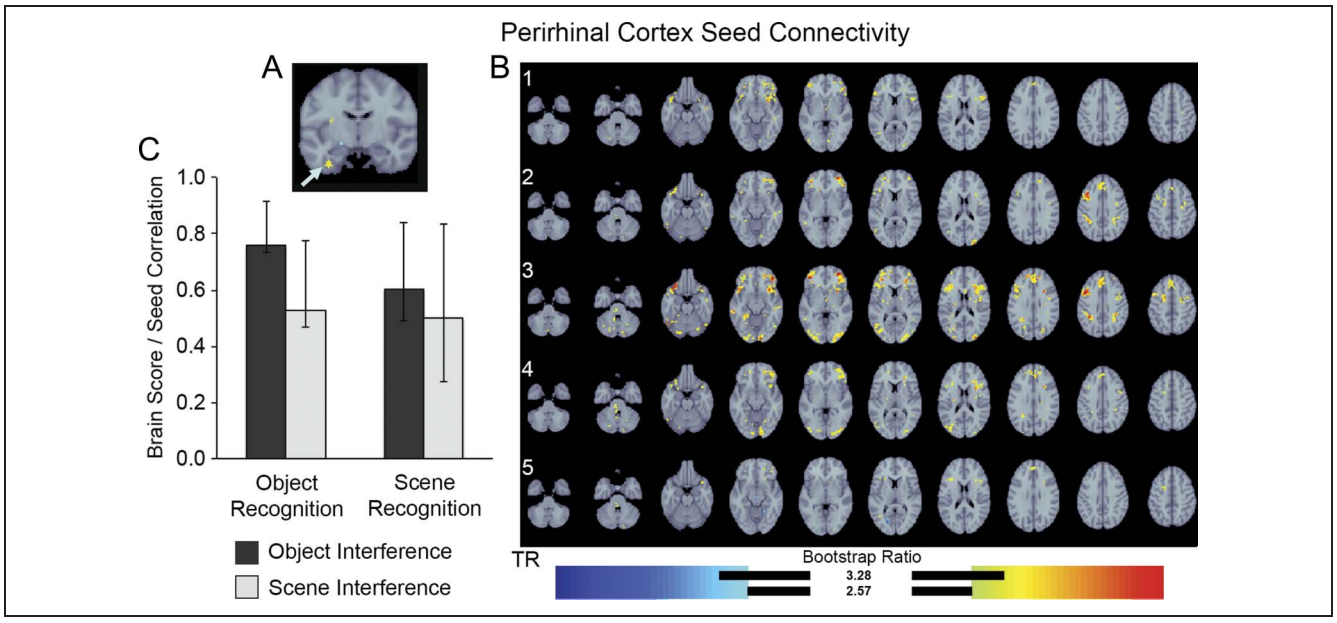

Figure 4. Seed PLS findings. (A) PRC seed region identified from the third lag of the critical LV shown in Figure 3. (B) Pattern of functional connectivity between the PRC seed and the regions contributing to the pattern shown in Figure 3B. (C) Brain score/seed correlations across experimental conditions. Note that the 95% CI bars overlap across conditions. Statistical map thresholded at BSR = 2.57 for presentation purposes. Brain images displayed using neurological convention (Left = Left).

and condition from the region identified in LV2 (i.e., −32, −10, −38; Figure 4A). A mask was applied to restrict the functional connectivity analysis to regions sensitive to the interference effect identified in LV2. This mask included regions expressed in any lag of LV2, using a liberal BSR of >2.16 or <−2.16, to maximize inclusion of regions differentiated by our object interference effect (i.e., those regions presented in hot or cool colors in Figure 3). As with the task PLS analyses, resulting correlation maps were analyzed with singular value decomposition to create LVs, each containing a singular value, a linear contrast between conditions and singular image detailing individual voxel saliences across the five lags. Furthermore, the significance of these LVs was assessed using a permutation method (500 permutations, $p < .05$), and the reliability of the voxel saliences from the resulting singular images was computed using 100 bootstraps for estimation of *SE* (BSR = 2.81).

Assessment of the functional connectivity between the seed and interference-related regions identified a significant LV ($p < .0001$; see Figure 4B and C). Similar to the design scores from the task PLS analysis, the direction and magnitude of the correlation values plotted in Figure 4C reveal the per-condition functional connectivity between the PRC seed and the observed pattern of brain activity for the LV. This analysis did not reveal differential contributions of the experimental conditions to the pattern of functional connectivity. Instead, similarly robust connectivity was present across all four IMTS conditions. Thus, although PRC and regions included in our mask were preferentially involved in the resolution of congruent interference during object recognition, the connectivity between PRC and these regions was not uniquely expressed in response to the effects of congruent interference during object recognition. Regions exhibiting reliable functional connectivity to the PRC seed (BSR > 2.81) are shown in warm colors in Figure 4B. Several of these peak saliences were present in regions predicted to support representation of visual information under conditions of interference: Lag 1, mid- (−52, 26, 8; BSR = 4.28) and anterior VLPFC (50, 30, −8.0; BSR = 5.64); Lag 3 rostral PFC (32, 54, 0; BSR = 8.62), anterior PRC (24, 8, −26; BSR = 7.37), DLPFC (−44, 12, 38; BSR = 7.63), ACC (4, 32, 44; BSR = 6.33), PPC (−22, −70, 30; BSR = 3.77), hippocampus (28, −20, −6; BSR = 4.44); Lag 5, mid-VLPFC (42, 18, 14; BSR = 5.00).

In summary, our neuroimaging findings revealed, using a data-driven approach, a pattern of brain regions that distinguished object and scene recognition. Interestingly, those regions recruited during object recognition (including PRC) contributed to a greater degree following congruent rather than incongruent interference, whereas the converse was not the case for the scene recognition condition. Assessment of the functional connectivity of PRC across recognition and interference manipulations did not reveal distinctions, suggesting that the increased contribution of PRC for object recognition following congruent interference is not due to specific recognition and interference conditions giving rise to a unique interplay between PRC and the rest of the brain. This provides a broader neural context for the key finding reported by Watson and Lee (2013)—greater univariate activation in PRC following congruent as compared to incongruent interference for object but not scene recognition. The forced-choice nature of our task, however, raises the question of whether the recruitment of this network primarily reflects assessment of the target images, or alternatively, the foil images. Disproportionate viewing of target or foil images could potentially shed light on the underlying recognition strategy, with greater viewing of foil images compared to targets before accurate recognition possibly reflecting a successful rejection of the foil, whereas greater viewing of target images compared to foils before accurate recognition could potentially reflect successful identification of the target. To shed some light on these issues, we assessed gaze duration during recognition to explore the consequences of visual interference on recognition memory decisions.

Eye-tracking Study

Behavioral Data

Figure 5A displays average MTS performance separated according to recognition condition from the eye-tracking participants. In all conditions, target versus foil MTS discrimination was above chance (ts > 14, ps < .001). To test for differing effects of interference on memory, MTS accuracy for the four conditions was examined in a 2 × 2 within-subject ANOVA modeling factors of Interference and Memory. Results indicated a reliable interaction between these two factors ($F(1, 22) = 69.45$, $p < .001$). Follow-up tests (Bonferroni-corrected $p = .025$) revealed inferior performance following congruent interference as compared with incongruent interference in both the object recognition task (OROI < ORSI: $t(22) = 8.93$, $p < .001$) and the scene recognition task (SRSI < SROI: $t(22) = 4.12$, $p < .001$). This pattern of behavioral findings replicated those in the previously reported fMRI study (Watson & Lee, 2013).

Examination of 1-back behavioral data indicated that participants were attending to the interfering stimuli (each $d' > .99$; Figure 5B). These d' scores were submitted to a 2 × 2 ANOVA with factors of Recognition (scene vs. object) and Interference (scene vs. object). The d' performance in the eye-tracking participants revealed a main effect of Interference ($F(1, 22) = 44.35$, $p < .001$), reflecting higher d' values associated with object interference conditions. A direct comparison of object and scene interference conditions confirmed greater overall working memory performance for object compared with scene interference trials ($t(22) = 6.66$, $p < .001$). Again, this overall pattern is consistent with the findings of Watson and Lee (2013).

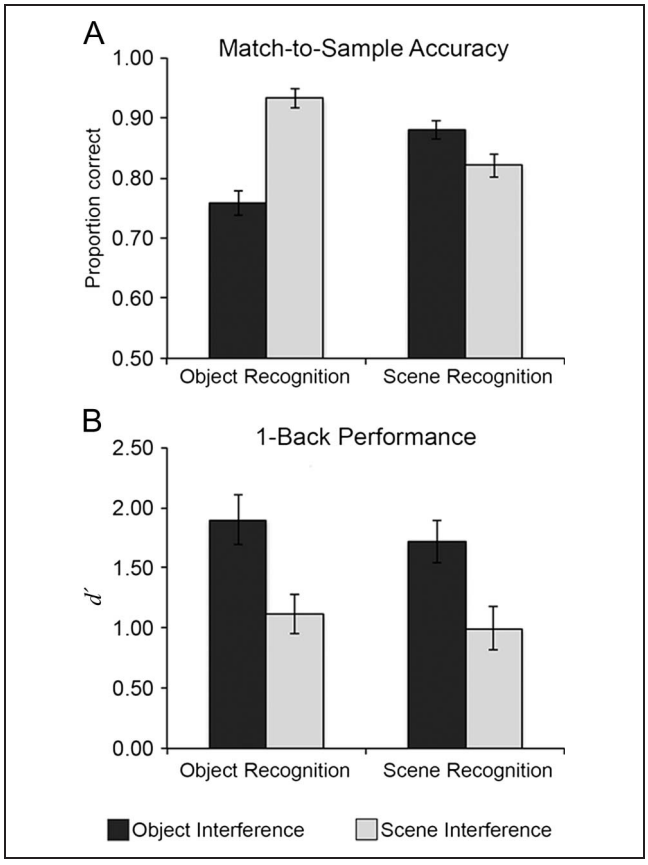

Figure 5. Behavioral performance of the eye-tracking experiment. (A) MTS accuracy for the four experimental conditions, indicating a sensitivity of object recognition to interference type. (B) 1-Back image repetition detection performance for the four experimental conditions. Positive d' scores indicate that participants were attending to interfering stimuli. Error bars denote *SEM*.

Eye-tracking Data

To assess the effects of congruent and incongruent interference, target–foil viewing bias was calculated for recognition memory conditions (object or scene), separately by Interference type and Accuracy. Although the examination of Interference type, Recognition type, and Accuracy did not reveal a three-way interaction ($F(1, 22) = 2.29, p = .14$), given our a priori goal of comparing the effects of interference during scene and object interference, we explored the data further by examining these memory conditions separately using 2 × 2 (Accuracy × Interference) ANOVAs. This approach allowed assessment of the effects of congruent and incongruent interference on discrimination, which is determined by the nature of the stimulus being discriminated at test. Both ANOVAs revealed a main effect of Accuracy on viewing bias (Object memory: $F(1, 22) = 37.40, p < .001$; Scene memory: $F(1, 22) = 28.38, p < .001$). These main effects reflected a greater tendency to view the item subsequently selected, with increased viewing of the target (positive bias values) for correct trials and increased viewing of the foil (negative bias values) for incorrect trials (Figure 6).

The main effect of Interference for either recognition condition was not significant (Object memory: $F(1, 22) = .67$, $p > .40$; Scene memory: $F(1, 22) = .16, p > .60$). Notably, although the factors of accuracy and interference did not interact for the Scene recognition conditions ($F(1, 22) = .002, p > .9$; Figure 6B), these factors did interact for the Object recognition conditions ($F(1, 22) = 6.80, p < .05$; Figure 6A), suggesting eye movements during object recognition were differentially impacted by congruency of visual interference. Planned comparisons of the object recognition trials revealed that viewing bias was modulated by interference congruency, with a greater target viewing bias following object as compared to scene interference ($t(22) = 2.39, p < .05$) on correct trials and increased foil viewing on incorrect trials following object as compared to scene interference ($t(22) = 2.06, p < .05$; Figure 6A). Interference type did not modulate viewing bias in the scene recognition condition (all ps > .25; Figure 6B). To explore the data further, an inspection of the raw PVT data using planned comparisons revealed that object recognition following object interference was

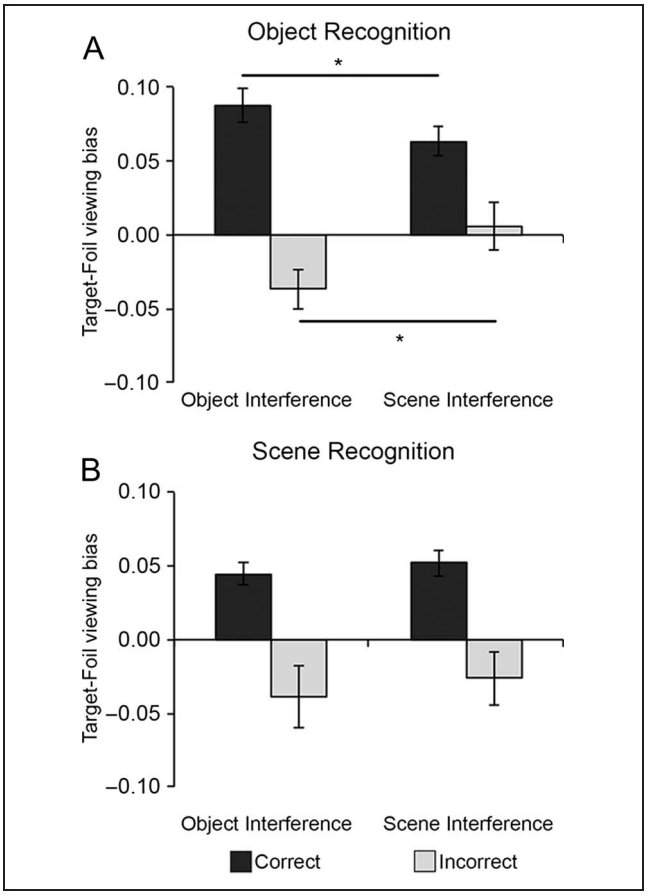

Figure 6. Target > foil viewing biases, expressed as a difference in PVT during test. Positive values indicate a greater tendency to view target images, whereas negative values indicated a greater tendency to view at foil images. (A) Viewing biases during object recognition trials. (B) Viewing biases during scene recognition trials. Asterisks denote that object, but not scene, recognition was sensitive to interference type ($p < .05$). Error bars display *SEM*.

associated with greater viewing of targets on correct as compared to incorrect trials ($t(21) = 4.31$, $p < .001$) and greater viewing of foils on incorrect as compared to correct trials ($t(21) = 4.09$, $p < .001$), consistent with the notion that gaze times can be impacted by congruent interference, perhaps through the induction of a false sense of familiarity for foil items. Incongruent interference did not, however, have the same effect on object recognition trials, with scene interference failing to bias viewing times for object recognition trials; similar PVTs for targets on correct and incorrect object recognition trials were revealed following scene interference ($t(13) = 1.56$, $p > .14$), as was the case for foil stimuli ($t(14) = .50$, $p > .60$). Thus, our eye-tracking findings paralleled our neuroimaging findings, in that object, but not scene recognition, was impacted by the congruency of interference.

DISCUSSION

Previous work has highlighted a role for PRC in support of object recognition following periods of congruent visual interference but has not assessed the effects of changing recognition and interference demands on other brain regions known to contribute to interference resolution. To address this, we used a forced-choice recognition task to examine the impact of congruent and incongruent visual interference in two ways. First, we examined the interplay between PRC and regions known to support executive processing demands necessary for overcoming mnemonic interference. As predicted, a data-driven fMRI analysis approach revealed a reliable pattern of activity associated with object recognition following congruent interference. Consistent with the findings of Watson and Lee (2013), this pattern included PRC as well as regions known to support executive processing during memory decisions, including VLPFC, DLPFC, PPC, and ACC. Although these regions were preferentially engaged during object recognition following congruent interference, functional connectivity between these regions was similar across recognition and interference conditions, pointing to a more general role in interference resolution. Second, we used eye tracking in a separate behavioral experiment to examine the impact of interference on the viewing of simultaneously presented target and foil images. This approach revealed that the congruency of the interference type differentially affected viewing bias for object but not scene recognition. Following congruent interference, participants had a greater tendency to view targets before accurate object recognition judgments and lures before inaccurate recognition decisions. This viewing pattern is consistent with object interference generating a false sense of familiarity for the lure image. Together, our neuroimaging and eye-tracking results suggest that the recognized contributions of PRC to object recognition following periods of visual interference reflect a broader co-recruitment of executive functioning regions and that congruent interference not only preferentially activates this network of regions but is also associated with a gaze duration profile that is distinct from that associated with scene recognition demands.

The pattern of activity revealed by our data-driven PLS analysis uncovered two significant LVs. The first LV differentiated experimental conditions by interference type. Critically, this effect was predominately driven by incongruent interference conditions. Examining the pattern of brain regions exhibiting this effect revealed greater activation in regions known to be category-selective for the stimulus being discriminated (including lateral occipital cortex and parahippocampal cortex for objects and scenes, respectively). This may reflect greater access to information in the relevant domain following periods of reduced (irrelevant) interference. Consistent with this interpretation, behavioral performance was elevated in the incongruent interference conditions that contributed most strongly to this pattern.

The second LV differentiated object and scene recognition conditions, primarily driven by a strong pattern of activity expressed following congruent interference. This pattern included PRC but, more critically, also revealed a broader network of regions known to contribute to the selection and retrieval of information under conditions of interference. We interpret co-recruitment of these regions (DLPFC, VLPFC, ACC, and PPC) as reflecting the consequences of congruent visual interference on recognition decisions for objects. In the context of a forced-choice recognition task, congruent periods of visual interference, either through the presentation of highly similar items during the delay period or through the presentation of highly similar foils at test (or the contributions of both as in the current study) increases the activation strength of irrelevant competitors. These competing representations create conflict when attempting to identify the target item, and place an emphasis on PFC-dependent retrieval monitoring and post-retrieval selection processes that enable the filtering and selection of goal relevant from irrelevant retrieved representations (Hayama & Rugg, 2009; Thompson, Cusack, & Duncan, 2009; Petrides, 2002; Petrides, Alivisatos, & Frey, 2002; Miller & Cohen, 2001; Cohen, Dunbar, & McClelland, 1990).

Notably, the pattern of activity that differentiated the congruent object interference condition from the other experimental conditions also included the hippocampus. Interference demands may have resulted in an increased reliance of pattern separation-related processing in the hippocampus and/or match/mismatch sensitivity in the support of recognition. This pattern of findings was not revealed in previous univariate analyses of the data, perhaps because of the reduced sensitivity of the univariate analysis approach with respect to small but reliable changes in activity (McIntosh & Lobaugh, 2004). Scene recognition, on the other hand, was associated with greater involvement of the parahippocampal gyrus around the third lag, with little reliable coactivity with prefrontal regions, consistent with the notion that scene

familiarity may rely upon a different neural substrate than object familiarity (Martin, McLean, O'Neil, & Köhler, 2013). Importantly, the pattern displayed in the second LV does not indicate that there is an absence of prefrontal contributions during scene recognition, rather that coactivation of PRC with prefrontal regions during object recognition is more reliable.

One possible interpretation of the increased recruitment of regions supporting monitoring and selection during the OROI condition is that, numerically, performance was the worst in this condition. We view task difficulty as unlikely to fully explain our pattern of findings given that, aside from the congruent object recognition condition, the pattern of behavioral findings does not map on to the LV revealed by our PLS analysis. More specifically, if difficulty were primarily responsible for the effects reported here, one would expect a pattern of activity differentiating congruent from incongruent interference conditions, irrespective of domain. Instead, the second LV differentiates conditions primarily on the basis of scene/object recognition conditions.

Our seed-based PLS analysis revealed significant functional connectivity between PRC and a number of the regions identified in LV2 of our task PLS analysis, including the DLPFC, VLPFC, PPC, and ACC. Significant PRC functional connectivity with a number of these regions converges with previous resting state studies that have examined PRC connectivity under task-free conditions. These investigations have revealed connectivity between PRC and a network that includes medial and lateral temporal regions (Libby, Ekstrom, Ragland, & Ranganath, 2012; Kahn, Andrews-Hanna, Vincent, Snyder, & Buckner, 2008) as well as ventral aspects of PFC (Libby et al., 2012). Notably, however, we found a wider pattern of connectivity associated with the recognition memory demands of the current study, not dissimilar to other studies that have observed broader PRC connectivity during task conditions than those identified during resting state scanning. For example, O'Neil et al. (2011) examined connectivity differences for perceptual and recognition tasks involving faces and found increased PRC connectivity with ACC as well as VLPFC, similar to the current study. In addition, McLelland, Chan, Ferber, and Barense (2014) revealed PRC connectivity centered primarily in occipital and lateral temporal regions during familiar as compared to unfamiliar object and face presentation. Although our design does not permit differential interpretation of lateral prefrontal and cingulate contributions, given their common recruitment, our findings highlight the interplay between the MTL and these regions which have been implicated in interference resolution. The broader connectivity of the PRC under task conditions, emphasizing frontal and parietal contributions related to the resolution of visual interference, is in line with previous research and consistent with theories positing that the PRC can support representations that aid in the resolution of visual interference (Graham, Barense, & Lee, 2010; Bussey & Saksida, 2007; Murray et al., 2007). Although these findings indicate interplay between PFC and MTL in the service of recognition under interference demands, more work is needed to tease apart the role of specific PFC subregions and the consequence of functional connectivity of the MTL on these subregions with respect to mnemonic and executive processing demands.

Interestingly, PRC was not found to exhibit distinct patterns of functional connectivity across our experimental conditions. Instead, a consistent profile of functional connectivity was present despite differential involvement of this network under conditions of object recognition following congruent interference (task PLS analysis, LV2), suggesting a more robust recruitment of a generalized network supporting the resolution of perceptual interference in the service of recognition memory. Similar connectivity across conditions raises the question of why this network was differentially recruited during object recognition following object interference. One possibility is that this network supports object interference resolution when monitoring demands are elevated (i.e., following congruent interference) but is nevertheless recruited, albeit to a lesser degree, when monitoring demands are reduced through incongruent interference or during scene recognition, which may rely less on networks that include PRC. PRC is often implicated to a greater extent in object recognition as compared to scene recognition (as reviewed in Ranganath & Ritchey, 2012; Diana, Yonelinas, & Ranganath, 2007; Eichenbaum, Yonelinas, & Ranganath, 2007; Davachi, 2006). For instance, a recent multivariate pattern analysis study has suggested that familiarity for objects may be supported by PRC-based representations, with scene recognition supported by the parahippocampal cortex (Martin et al., 2013), in line with the univariate findings reported by Watson and Lee (2013). Thus, differential recruitment of the network reported in this study following congruent and incongruent interference conditions for object, but not scene, recognition is in agreement with the view that the former is supported to a greater extent by PRC, whereas the latter is supported to a greater extent by parahippocampal cortex.

Eye-tracking analyses revealed a tendency for participants to view the item that they subsequently selected, but closer inspection of the data revealed an interference effect that paralleled the neuroimaging data. Eye movements were impacted by the nature of the interference in the object recognition condition. Specifically, participants had a greater tendency to look at lures before making an object recognition error following congruent as compared to incongruent interference. This finding, which was not present for scene recognition, suggests that object interference may have created a higher level of false familiarity for foil items in comparison to scene interference. Previous eye-tracking work also points to the possibility that object interference during visual object recognition can lead to foils appearing familiar. Specifically, Yeung et al. (2013) found that patients at risk for mild cognitive

impairment (MCI) demonstrated increased vulnerability to visual interference, as measured by eye movements, compared to neurologically healthy controls during a passive serial viewing task. These individuals exhibited a reduction in fixation number when viewing novel objects similar to those seen previously as compared to other novel objects which were less visually similar, suggesting that the former were perceived as familiar by the participant. Thus, changes associated with MCI may impact the vulnerability of recognition processes to feature interference, contributing to forgetting.

Although the impact of congruent interference on object recognition was expected, the similar pattern of gaze duration for congruent and incongruent interference during scene recognition was not anticipated. One potential contributing factor to this is differential processing of the object and scene interfering information as a result of the manner in which the objects/scenes were presented and the amount of inherent semantic information that they contained. Whereas the object interfering stimuli were common, namable items presented in the foreground, the scene interfering stimuli were novel scenes that possessed relatively little semantic content and were presented as background images. Subsequently, basic level object identity and the increased saliency of foreground information may have underpinned one-back performance during object interference. In contrast, the scenes may have been processed at a relatively shallower level, with scene 1-back performance relying to a greater extent on lower-level visual information. Indeed, 1-back performance was greater for objects than scenes. Thus, factors impacting automatic processing of stimuli, such as semantic content, may also impact sensitivity to visual interference.

In summary, our findings support a role of the MTL in interference resolution and suggest that PRC may support representations that can aid object discrimination. Notably our current findings go beyond previous demonstrations of PRC involvement in object memory tasks by exploring the interplay between the MTL and the rest of the brain under varying interference and recognition demands. To this end, we observed that PRC coactivates PFC and PPC regions in support of controlled retrieval and response selection. Moreover, although one might expect that demands associated with object recognition following object interference may invoke distinct connectivity between PRC and prefrontal/parietal areas, given that activation of this region is elevated under these conditions, this was not found to be the case. Instead, an examination of varying object and scene recognition/interference demands revealed a stable pattern of functional connectivity. This intriguing finding suggests that while being particularly relevant to conditions of high object feature interference, this network of brain areas is also deployed under a variety of feature interference conditions, providing important insight into the contexts under which PRC contributes to interference resolution. Finally, our eye-tracking findings suggest that eye movements can shed light on the nature of the visual information used to support item discrimination and that patterns of eye movements can reflect the impact of recent visual experience on visual recognition. Together, our neuroimaging and eye-tracking data point to a role of an extended network of regions in the support of recognition following periods of interference and point to role of PRC in the support of object representations that reflect the consequences of visual interference (Cowell et al., 2010; Bussey & Saksida, 2007; Murray et al., 2007).

Acknowledgments

This work was supported by the Natural Sciences and Engineering Research Council of Canada (grants 412309-2011 and 402651-2011 to A. C. H. L.) and the Wellcome Trust, UK (grant 082315 to A. C. H. L.). The authors thank all the participants for their time and Dr. Sarah J. Miles for statistical advice.

Reprint requests should be sent to Dr. Edward B. O'Neil, Department of Psychology, University of Toronto Scarborough, 1265 Military Trail, Toronto, Ontario, M1C 1A4, Canada, or via e-mail: edoneil@gmail.com.

REFERENCES

Anderson, M. C., & Spellman, B. A. (1995). On the status of inhibitory mechanisms in cognition: Memory retrieval as a model case. *Psychological Review, 102,* 68–100.

Axmacher, N., Schmitz, D. P., Wagner, T., Elger, C. E., & Fell, J. (2008). Interactions between medial temporal lobe, prefrontal cortex, and inferior temporal regions during visual working memory: A combined intracranial EEG and functional magnetic resonance imaging study. *Journal of Neuroscience, 28,* 7304–7312.

Badre, D., Poldrack, R. A., Paré-Blagoev, E. J., Insler, R. Z., & Wagner, A. D. (2005). Dissociable controlled retrieval and generalized selection mechanisms in ventrolateral prefrontal cortex. *Neuron, 47,* 907–918.

Badre, D., & Wagner, A. D. (2002). Semantic retrieval, mnemonic control, and prefrontal cortex. *Behavioral and Cognitive Neuroscience Reviews, 1,* 206–218.

Badre, D., & Wagner, A. D. (2007). Left ventrolateral prefrontal cortex and the cognitive control of memory. *Neuropsychologia, 45,* 2883–2901.

Barense, M. D., Groen, I. I. A., Lee, A. C. H., Yeung, L.-K., Brady, S. M., Gregori, M., et al. (2012). Intact memory for irrelevant information impairs perception in amnesia. *Neuron, 75,* 157–167.

Barredo, J., Öztekin, I., & Badre, D. (2015). Ventral fronto-temporal pathway supporting cognitive control of episodic memory retrieval. *Cerebral Cortex, 25,* 1004–1019.

Bartko, S. J., Cowell, R. A., Winters, B. D., Bussey, T. J., & Saksida, L. M. (2010). Heightened susceptibility to interference in an animal model of amnesia: Impairment in encoding, storage, retrieval—Or all three? *Neuropsychologia, 48,* 2987–2997.

Beckmann, C. F., & Smith, S. M. (2004). Probabilistic independent component analysis for functional magnetic resonance imaging. *IEEE Transactions on Medical Imaging, 23,* 137–152.

Blumenfeld, R. S., Nomura, E. M., Gratton, C., & D'Esposito, M. (2013). Lateral prefrontal cortex is organized into parallel

dorsal and ventral streams along the rostro-caudal axis. *Cerebral Cortex, 23,* 2457–2466.
Blumenfeld, R. S., & Ranganath, C. (2007). Prefrontal cortex and long-term memory encoding: An integrative review of findings from neuropsychology and neuroimaging. *The Neuroscientist, 13,* 280–291.
Bunge, S. A., Hazeltine, E., Scanlon, M. D., Rosen, A. C., & Gabrieli, J. D. E. (2002). Dissociable contributions of prefrontal and parietal cortices to response selection. *Neuroimage, 17,* 1562–1571.
Bussey, T. J., & Saksida, L. M. (2002). The organization of visual object representations: A connectionist model of effects of lesions in perirhinal cortex. *European Journal of Neuroscience, 15,* 355–364.
Bussey, T. J., & Saksida, L. M. (2007). Memory, perception, and the ventral visual-perirhinal-hippocampal stream: Thinking outside of the boxes. *Hippocampus, 17,* 898–908.
Cohen, J. D., Dunbar, K., & McClelland, J. L. (1990). On the control of automatic processes: A parallel distributed processing account of the Stroop effect. *Psychological Review, 97,* 332–361.
Cowan, N., Beschin, N., & Della Sala, S. (2004). Verbal recall in amnesiacs under conditions of diminished retroactive interference. *Brain, 127,* 825–834.
Cowell, R. A., Bussey, T. J., & Saksida, L. M. (2006). Why does brain damage impair memory? A connectionist model of object recognition memory in perirhinal cortex. *Journal of Neuroscience, 26,* 12186–12197.
Cowell, R. A., Bussey, T. J., & Saksida, L. M. (2010). Functional dissociations within the ventral object processing pathway: Cognitive modules or a hierarchical continuum? *Journal of Cognitive Neuroscience, 22,* 2460–2479.
Davachi, L. (2006). Item, context and relational episodic encoding in humans. *Current Opinion in Neurobiology, 16,* 693–700.
de Zubicaray, G. I., McMahon, K., Wilson, S. J., & Muthiah, S. (2001). Brain activity during the encoding, retention, and retrieval of stimulus representations. *Learning & Memory, 8,* 243–251.
Diana, R. A., Yonelinas, A. P., & Ranganath, C. (2007). Imaging recollection and familiarity in the medial temporal lobe: A three-component model. *Trends in Cognitive Sciences, 11,* 379–386.
Durston, S., Thomas, K. M., Worden, M. S., Yang, Y., & Casey, B. J. (2002). The effect of preceding context on inhibition: An event-related fMRI study. *Neuroimage, 16,* 449–453.
Eichenbaum, H. (2004). Hippocampus: Cognitive processes and neural representations that underlie declarative memory. *Neuron, 44,* 109–120.
Eichenbaum, H., Yonelinas, A. P., & Ranganath, C. (2007). The medial temporal lobe and recognition memory. *Annual Review of Neuroscience, 30,* 123–152.
Fletcher, P. C., & Henson, R. N. (2001). Frontal lobes and human memory: Insights from functional neuroimaging. *Brain, 124,* 849–881.
Graham, K. S., Barense, M. D., & Lee, A. C. H. (2010). Going beyond LTM in the MTL: A synthesis of neuropsychological and neuroimaging findings on the role of the medial temporal lobe in memory and perception. *Neuropsychologia, 48,* 831–853.
Hannula, D. E., & Ranganath, C. (2008). Medial temporal lobe activity predicts successful relational memory binding. *Journal of Neuroscience, 28,* 116–124.
Hannula, D. E., Ryan, J. D., Tranel, D., & Cohen, N. J. (2007). Rapid onset relational memory effects are evident in eye movement behavior, but not in hippocampal amnesia. *Journal of Cognitive Neuroscience, 19,* 1690–1705.
Hayama, H. R., & Rugg, M. D. (2009). Right dorsolateral prefrontal cortex is engaged during post-retrieval processing of both episodic and semantic information. *Neuropsychologia, 47,* 2409–2416.
Holm, L., Eriksson, J., & Andersson, L. (2008). Looking as if you know: Systematic object inspection precedes object recognition. *Journal of Vision, 8,* 14.1–14.7.
Howard, M. W., & Eichenbaum, H. (2013). The hippocampus, time, and memory across scales. *Journal of Experimental Psychology: General, 142,* 1211–1230.
Iacoboni, M., Woods, R. P., & Mazziotta, J. C. (1998). Bimodal (auditory and visual) left frontoparietal circuitry for sensorimotor integration and sensorimotor learning. *Brain, 121,* 2135–2143.
Jenkinson, M. (2003). Fast, automated, N-dimensional phase-unwrapping algorithm. *Magnetic Resonance in Medicine, 49,* 193–197.
Jenkinson, M., Bannister, P., Brady, M., & Smith, S. (2002). Improved optimization for the robust and accurate linear registration and motion correction of brain images. *Neuroimage, 17,* 825–841.
Jenkinson, M., & Smith, S. (2001). A global optimisation method for robust affine registration of brain images. *Medical Image Analysis, 5,* 143–156.
Jezzard, P., & Balaban, R. S. (1995). Correction for geometric distortion in echo planar images from B0 field variations. *Magnetic Resonance in Medicine, 34,* 65–73.
Johnson, M. K., Raye, C. L., Mitchell, K. J., Greene, E. J., Cunningham, W. A., & Sanislow, C. A. (2005). Using fMRI to investigate a component process of reflection: Prefrontal correlates of refreshing a just-activated representation. *Cognitive, Affective & Behavioral Neuroscience, 5,* 339–361.
Kahn, I., Andrews-Hanna, J. R., Vincent, J. L., Snyder, A. Z., & Buckner, R. L. (2008). Distinct cortical anatomy linked to subregions of the medial temporal lobe revealed by intrinsic functional connectivity. *Journal of Neurophysiology, 100,* 129–139.
Kumaran, D., & Maguire, E. A. (2006). An unexpected sequence of events: Mismatch detection in the human hippocampus. *PLoS Biology, 4,* 2372–2382.
Libby, L. A., Ekstrom, A. D., Ragland, J. D., & Ranganath, C. (2012). Differential connectivity of perirhinal and parahippocampal cortices within human hippocampal subregions revealed by high-resolution functional imaging. *Journal of Neuroscience, 32,* 6550–6560.
MacDonald, A. W., Cohen, J. D., Stenger, V. A., & Carter, C. S. (2000). Dissociating the role of the dorsolateral prefrontal and anterior cingulate cortex in cognitive control. *Science, 288,* 1835–1838.
Martin, C. B., McLean, D. A., O'Neil, E. B., & Köhler, S. (2013). Distinct familiarity-based response patterns for faces and buildings in perirhinal and parahippocampal cortex. *Journal of Neuroscience, 33,* 10915–10923.
McCormick, C., Moscovitch, M., Protzner, A. B., Huber, C. G., & McAndrews, M. P. (2010). Hippocampal-neocortical networks differ during encoding and retrieval of relational memory: Functional and effective connectivity analyses. *Neuropsychologia, 48,* 3272–3281.
McIntosh, A. R., Bookstein, F. L., Haxby, J. V., & Grady, C. L. (1996). Spatial pattern analysis of functional brain images using partial least squares. *Neuroimage, 3,* 143–157.
McIntosh, A. R., & Lobaugh, N. (2004). Partial least squares analysis of neuroimaging data: Applications and advances. *Neuroimage, 23,* S250–S263.
McLelland, V. C., Chan, D., Ferber, S., & Barense, M. D. (2014). Stimulus familiarity modulates functional connectivity of the perirhinal cortex and anterior hippocampus during visual

discrimination of faces and objects. *Frontiers in Human Neuroscience, 8,* 117.
McTighe, S. M., Cowell, R. A., Winters, B. D., Bussey, T. J., & Saksida, L. M. (2010). Paradoxical false memory for objects after brain damage. *Science, 330,* 1408–1410.
Milham, M. P., & Banich, M. T. (2005). Anterior cingulate cortex: An fMRI analysis of conflict specificity and functional differentiation. *Human Brain Mapping, 25,* 328–335.
Milham, M. P., Erickson, K. I., Banich, M. T., Kramer, A. F., Webb, A., Wszalek, T., et al. (2002). Attentional control in the aging brain: Insights from an fMRI study of the Stroop task. *Brain and Cognition, 49,* 277–296.
Miller, E. K., & Cohen, J. D. (2001). An integrative theory of prefrontal cortex function. *Annual Review of Neuroscience, 24,* 167–202.
Murray, E. A., Bussey, T. J., & Saksida, L. M. (2007). Visual perception and memory: A new view of medial temporal lobe function in primates and rodents. *Annual Review of Neuroscience, 30,* 99–122.
Nee, D. E., Jonides, J., & Berman, M. G. (2007). Neural mechanisms of proactive interference-resolution. *Neuroimage, 38,* 740–751.
Nee, D. E., Wager, T. D., & Jonides, J. (2007). Interference resolution: Insights from a meta-analysis of neuroimaging tasks. *Cognitive, Affective & Behavioral Neuroscience, 7,* 1–17.
O'Neil, E. B., Protzner, A. B., McCormick, C., McLean, D. A., Poppenk, J., Cate, A. D., et al. (2011). Distinct patterns of functional and effective connectivity between perirhinal cortex and other cortical regions in recognition memory and perceptual discrimination. *Cerebral Cortex, 22,* 74–85.
Pardo, J. V., Pardo, P. J., Janer, K. W., & Raichle, M. E. (1990). The anterior cingulate cortex mediates processing selection in the Stroop attentional conflict paradigm. *Proceedings of the National Academy of Sciences, 87,* 256–259.
Petrides, M. (2002). The mid-ventrolateral prefrontal cortex and active mnemonic retrieval. *Neurobiology of Learning and Memory, 78,* 528–538.
Petrides, M., Alivisatos, B., & Frey, S. (2002). Differential activation of the human orbital, mid-ventrolateral, and mid-dorsolateral prefrontal cortex during the processing of visual stimuli. *Proceedings of the National Academy of Sciences, U.S.A., 99,* 5649–5654.
Praamstra, P., Kleine, B. U., & Schnitzler, A. (1999). Magnetic stimulation of the dorsal premotor cortex modulates the Simon effect. *NeuroReport, 10,* 3671–3674.
Ranganath, C., & D'Esposito, M. (2005). Directing the mind's eye: Prefrontal, inferior and medial temporal mechanisms for visual working memory. *Current Opinion in Neurobiology, 15,* 175–182.
Ranganath, C., & Ritchey, M. (2012). Two cortical systems for memory-guided behaviour. *Nature Reviews Neuroscience, 13,* 713–726.
Ryan, J. D., Hannula, D. E., & Cohen, N. J. (2007). The obligatory effects of memory on eye movements. *Memory, 15,* 508–525.
Saksida, L. M., & Bussey, T. J. (2010). The representational–hierarchical view of amnesia: Translation from animal to human. *Neuropsychologia, 48,* 2370–2384.
Smith, S. M. (2002). Fast robust automated brain extraction. *Human Brain Mapping, 17,* 143–155.
Smith, S. M., Jenkinson, M., Woolrich, M. W., Beckmann, C. F., Behrens, T. E. J., Johansen-Berg, H., et al. (2004). Advances in functional and structural MR image analysis and implementation as FSL. *Neuroimage, 23(Suppl. 1),* S208–S219.
Stevens, W. D., Hasher, L., Chiew, K. S., & Grady, C. L. (2008). A neural mechanism underlying memory failure in older adults. *Journal of Neuroscience, 28,* 12820–12824.
Thompson, R., Cusack, R., & Duncan, J. (2009). Top–down activation of shape-specific population codes in visual cortex during mental imagery. *Journal of Neuroscience, 29,* 1565–1572.
Thompson-Schill, S. L., D'Esposito, M., Aguirre, G. K., & Farah, M. J. (1997). Role of left inferior prefrontal cortex in retrieval of semantic knowledge: A reevaluation. *Proceedings of the National Academy of Sciences, U.S.A., 94,* 14792–14797.
Tomita, H., Ohbayashi, M., Nakahara, K., Hasegawa, I., & Miyashita, Y. (1999). Top–down signal from prefrontal cortex in executive control of memory retrieval. *Nature, 401,* 699–703.
Warren, D. E., Duff, M. C., Tranel, D., & Cohen, N. J. (2011). Observing degradation of visual representations over short intervals when medial temporal lobe is damaged. *Journal of Cognitive Neuroscience, 23,* 3862–3873.
Warrington, E. K., & Weiskrantz, L. (1970). Amnesic syndrome: Consolidation or retrieval? *Nature, 228,* 628–630.
Watson, H. C., & Lee, A. C. H. (2013). The perirhinal cortex and recognition memory interference. *Journal of Neuroscience, 33,* 4192–4200.
Yassa, M. A., & Stark, C. E. L. (2011). Pattern separation in the hippocampus. *Trends in Neurosciences, 34,* 515–525.
Yeung, L.-K., Ryan, J. D., Cowell, R. A., & Barense, M. D. (2013). Recognition memory impairments caused by false recognition of novel objects. *Journal of Experimental Psychology: General, 142,* 1384–1397.